J. Hydrol. Hydromech., 72, 2024, 4, 466–485
https://doi.org/10.2478/johh-2024-0021
© 2024 Jakub Jeřábek and Petr Kavka, published by Sciendo. This work is licensed under the Creative Commons Attribution-NonCommercial-NoDerivatives 4.0 International Licence.

sciendo Journal of Hydrology and Hydromechanics Institute of Hydrology SAS

Sensitivity and uncertainty analysis of a surface runoff model using ensemble of artificial rainfall experiments

Jakub Jeřábek*, Petr Kavka

The Department of Landscape Water Conservation, Faculty of Civil Engineering, Czech Technical University in Prague, Thákurova 7/2077, 166 29 Praha 6 – Dejvice, Czech Republic.
* Corresponding author. Tel.: +420224354570. E-mail: jakub.jerabek@fsv.cvut.cz

Abstract: Surface runoff models are essential for designing water and soil protection measures. However, they often exhibit uncertainty in both parameterization and results. Typically, uncertainty is evaluated by comparing model realizations with measured data. However, this approach is constrained by limited data availability, preventing comprehensive uncertainty assessment. To overcome this limitation, we employed the generalized likelihood uncertainty estimation (GLUE) methodology to conduct sensitivity and uncertainty analyses on a series of surface runoff models. These models were based on an ensemble of artificial rainfall experiments comprising 77 scenarios with similar settings. We utilized the rainfall-runoff-erosion model SMODERP2D to simulate the experiments and employed Differential Evolution, a heuristic optimization method, to generate sets of behavioural models for each experiment. Additionally, we evaluated the sensitivity and uncertainty with respect to two variables; water level and surface runoff. Our results indicate similar sensitivity of water level and surface runoff to most parameters, with a generally high equifinality. The ensemble of models revealed high uncertainty in bare soil models, especially under dry initial soil water conditions where the lag time for runoff onset was the largest (e.g. runoff coefficient ranged between 0–0.8). Conversely, models with wet initial soil water conditions exhibited lower uncertainty compared to those with dry initial soil water content (e.g. runoff coefficient ranged between 0.6 – 1). Models with crop cover showed a multimodal distribution in water flow and volume, possibly due to variations in crop type and growth stages. Therefore, distinguishing these crop properties could reduce uncertainty. Utilizing an ensemble of models for sensitivity and uncertainty analysis demonstrated its potential in identifying sources of uncertainty, thereby enhancing the robustness and generalizability of such analyses.

Keywords: Surface runoff model; Uncertainty analysis; Sensitivity analysis; GLUE; Model ensemble.

INTRODUCTION

Surface runoff is a critical phenomenon that affects soil quality via water erosion (Boardman and Poesen, 2006) and it is a major cause of soil material accumulation and pollution in water bodies, especially in agricultural areas (e.g., Carpenter et al., 1998). Prediction of surface water flow velocity is crucial to calculate the shear stress of overland flow, while prediction of water flow and volume is important to assess the amount of water and suspended sediment displaced during the rainfall-runoff episode. These types of prediction are subjected to uncertainty that should be evaluated prior to any modelling task even in practice (Benke et al., 2008; El Ghoul et al., 2023). Even though variables as water flow velocity and water volume are critical, they are rarely assessed simultaneously or are often studied only at small set of rainfall-runoff episodes or experiments that limit the uncertainty assessment.

The uncertainty in the hydrological model can be classified as uncertainty in model forcing (e.g., rainfall (Cluckie et al., 2006)), model parameters (e.g., Loosvelt et al., 2011), or model structure (Gupta and Govindaraju, 2023). Forcing uncertainty is hard to quantify, as modellers often lack information about epistemic errors (Beven and Binley, 2014). However, such types of errors may be overcome via using rainfall simulators, which provide more control over the rainfall parameters. Structural uncertainty reflects the simplifying nature of any model of the natural system and can be theoretically reduced by introducing new processes into the model. Parameter uncertainty that can originate from unknown spatial heterogeneity of soil hydraulic causes an evenly distributed soil water content that does not represent the reality (Li et al., 2021). The latter, cannot be assessed using single (or few) rainfall-runoff episode or experiments, since only one (or few) realization of the spatial heterogeneity is assessed. We hypothesized that using an ensemble of experiments the uncertainty that originates from spatial heterogeneity can be considered and reflected in the uncertainty in model results.

Generalized Likelihood Uncertainty Estimation, i.e., GLUE (Beven and Binley, 1992), is a common approach to assess both model sensitivity and uncertainty. It evaluates the behaviour of a model in terms of sets of parameters that produce either behavioural or non-behavioural simulations (Freer and Beven, 2000). In its basic form, GLUE utilizes a likelihood function derived from a model performance measure to assess the likelihood of given parameter set or given model results to uncertainty. GLUE originally uses Monte Carlo simulations to generate a set of models that are further used to infer the likelihood function. Alternatively, methods such as Monte Carlo Markov Chain (MCMC) (Blasone et al., 2008) or Differential Evolution Adaptive Metropolis (DREAM) (Vrugt et al., 2009) can be used to generate sets of behavioural models more efficiently, especially by reducing the autocorrelation time (Brunetti et al., 2019). In contrast to formal Bayesian analysis, the GLUE methodology does not require a parameterized statistical distribution to be defined (Gupta and Govindaraju, 2023). This allows the evaluation of uncertainty even when the statistical distribution is unknown, as is the case with epistemic errors (Beven and Binley, 2014). However, a limitation of GLUE is that it does not provide a complete uncertainty evaluation; it only assesses uncertainty within

the range of evaluated models – therefore using model ensemble with GLUE may help to generalize the calculated uncertainties.

GLUE has been used to assess uncertainty in various models and systems, including the kinematic wave approximation of overland flow model (Hantush and Kalin, 2005), the dual-permeability model (Dohnal et al., 2012), or large-scale sediment delivery models (Cho et al., 2022; Shen et al., 2012; Vigiak et al., 2006). Recently, GLUE was employed to estimate the uncertainty in discharge and model parameters resulting from different rainfall estimations (Nanding et al., 2021), or to assess the effects of land use and land cover changes on model uncertainty (El Ghoul et al., 2023). These examples show that GLUE is a versatile tool suitable for problems with various scales, types, and numbers of variables.

In model optimization problems, it was suggested that multiple model performance metrics or multiple observations may be used as a goodness of fit criterion. In some cases, the combination of soil water potential and volumetric water content data was shown to be successful in identifying unique parameter sets (Šimůnek and van Genuchten, 1996; Vrugt and Bouten, 2002). The multi-objective framework was used in several studies with combination of GLUE (Dohnal et al., 2012; Zhou et al., 2016). Although typically in multi-objective assessment a Pareto front is used to balance the trade of between the objectives (Turunen et al., 2020) a single objective function is often used in Bayesian or GLUE based uncertainty analysis (Moges et al., 2021).

The motivation of this work is to enhance our understanding of uncertainty and sensitivity in surface runoff and water flow velocity calculations. We based our approach on SMODERP1D model where soil particles with varying grain sizes were carefully deposited on the bottom of the flume in an extremely thin layer to specify model parameters (Holý, 1984; Vrána et al., 1996). This approach aimed to measure the model parameters as accurately as possible - reducing uncertainty. In contrast, in this paper, we utilize an ensemble of artificial rainfall experiments performed in the field that introduce uncertainty that originates from soil and vegetation properties into the assessment while keeping the forcing rainfall relatively certain. We assume that using an ensemble of artificial rainfall experiments rather than a single or few experiments, the uncertainty that originates in spatial variability of soil and vegetation properties can be revealed. By doing the sensitivity and uncertainty assessment of a single experiment (or episode), only one realization of the spatial variability of soil and vegetation properties would be evaluated.

The objectives of this study are to assess potential of using ensemble of artificial rainfall experiments to address model structure and model parameters uncertainty, that is caused by soil surface features not included in the model. Additionally, we aim to address the sensitivity and uncertainty in two variables – surface runoff and surface water flow velocity – that were independently measured during each of experiment. This throughout and novel sensitivity and uncertainty assessment can help potential users of such models to view model results in its complexity. This is particularly important in the case of public domain models such as SMODERP2D (github.com/storm-fsv-cvut/smoderp2d: SMODERP2D – Distributed event-based model for surface and subsurface runoff and erosion), the model used in presented study.

MATERIALS AND METHODS

The episodical rainfall-runoff-erosion SMODERP2D (Kavka et al., 2022) model was used to perform the uncertainty analysis (UA) and sensitivity analysis (SA) of the model according to GLUE methodology (Beven and Binley, 1992). Two types of variables, surface runoff and water level, obtained from ensemble of field rainfall experiments were used to perform the UA and SA. The differential evolution (DE) optimization method (Storn and Price, 1997) was used to generate set of behavioural models.

Site description

The study was carried out at the Řisuty experimental site, located approximately 30 km northwest of Prague, Czech Republic, at coordinates 50°13'2.0" N, 14°1'2.2" E (see Figure 1). The elevation of the site ranges from 310 to 315 meters above sea level. With an annual mean temperature of 8°C and mean annual precipitation of 500 mm, the climate is classified as humid continental. The topsoil was classified as loam with 18.3% clay, 33.8% silt and 47.9% sand and the soil type is Cambisol.

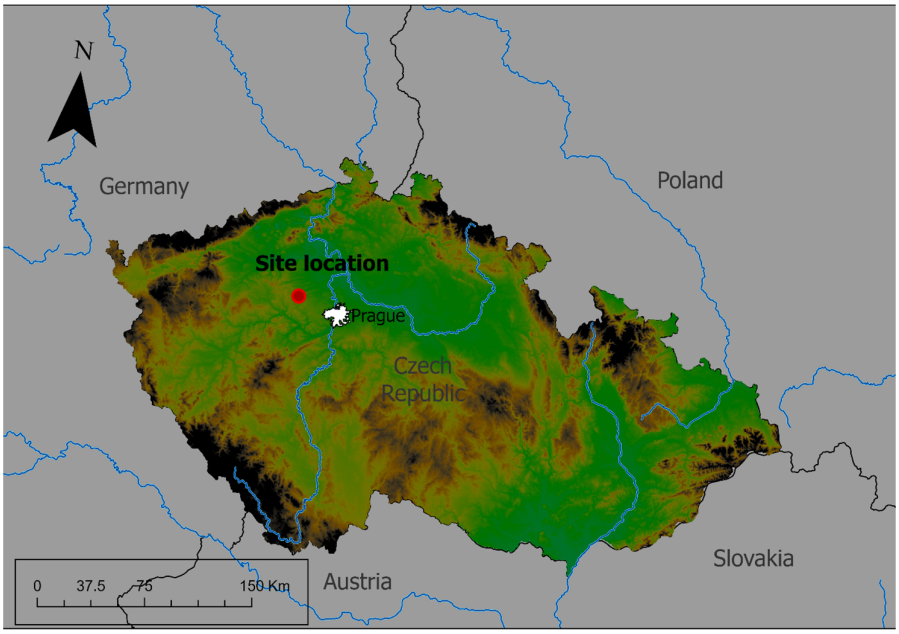

Fig. 1. Location of the experimental site.

Ensemble of artificial rainfall experiments

Series of artificial rainfall experiments (ARE) were performed using mobile field rainfall simulator (Kavka et al., 2018) on the experimental site between 2020 and 2022. The summary of the experiments used is shown in Table 1. A total of 77 experiments were used for optimization. 38 experiments were carried out under dry initial soil water content conditions and 39 under wet initial soil water content conditions. The pair of dry-wet experiments was always carried out sequentially with a break of 15 minutes, i.e., the dry initial conditions were caused by antecedent natural rainfall, the wet conditions were the conditions after the first 'dry' measurement. The dry experiments were not done immediately after natural rainfall. The field needed to be dry for the experimental setup to be transported and prepared. Soil surface conditions varied among the experiments. In total, 34 experiments were carried out on cultivated bare soil (defined below) and 43 on plots with cropped soil surface. The crop cover during the experiments is given in Table 2. Although different crop types and seeding schemes may have a potential effect on changes in surface runoff and water flow velocity (Wang et al., 2021), we only distinguish bare soil and vegetated soil for further analysis disregarding the effect of crop development on soil hydraulic properties (Schwen et al., 2011). The experimental data were extracted from "An open rainfall-runoff measurement database" (https://runoffdb.fsv.cvut.cz/en) (Devátý et al., 2020).

Table 1. The amount of artificial rainfall experiment conducted on different soil surface covers under different initial soil water content conditions.

		Initial SWC		
		Dry	Wet	Sum
Soil cover	Cultiv. bare soil	14	20	34
	Crop	24	19	43
	Sum	38	39	77

Rainfall simulation

A single ARE measurement was performed on a 16 m^2 plot with an average slope of 10%. All experiments were carried out with a rainfall intensity of approximately 60 mm/hour. Surface runoff was collected in plastic bottles at intervals of 1 to 2.5 minutes and then weighed to determine surface runoff volume. As part of post-processing, the surface runoff data was interpolated to 30-second intervals. The flow velocity of the surface water was measured with the dye tracer 2 to 4 times during each experiment. The velocity in the lowest section of the plot was recalculated to the average surface water level using surface runoff and the width of the plot (2 m). A typical rainfall experiment lasted 30 to 60 minutes, during which surface runoff was collected for 30 minutes. If no surface runoff occurred for 30 minutes, the experiment was stopped. In the following analysis, the 30 minutes since the start of the rainfall were used. Detailed information on the rainfall simulator used can be found in (Kavka et al., 2018).

The bare soil plot was prepared each time prior to measurement. The soil was first cultivated with a rototiller to a depth of approximately 12 cm. The surface was then further smoothed using rakes and by rolling a 50-liter cylinder filled with water. Consequently, the cultivated bare soil remained relatively consistent in all experiments.

All crops in the cropped plots were planted at the beginning of the vegetation season. Experiments were carried out over the period of plant growth, and the soil surface was not treated, except for the removal of wild vegetation using herbicides. Despite the potential varied effects of different crops and their growth stages on surface runoff generation, we do not distinguish between crop types and ages in the analysis. This approach allows us to assess the model's performance under vegetated conditions, implicitly considering the full range of crop variability.

SMODERP2D model

The episodic rainfall-runoff-erosion SMODERP2D model was used to conduct the sensitivity and uncertainty analysis. The 2D version of the model is based on 1D profile version where the surface runoff and erosion were calculated in multiple 1D profiles representing the main flow path in the hillslope (Dostál et al., 2000). The model was recently applied in rill development (Kavka et al., 2022) or surface runoff routing studies (Jeřábek et al., 2022). The current generation of the SMODERP2D model is implemented in Python to be compatible with most GIS software (Kavka et al., 2023).

The SMODERP2D model is primarily designed for surface runoff and erosion computation. Surface flow routing in the model is based on the digital elevation model (DEM). DEM also controls the spatial discretization of the model. In the case of this study, the resolution was 0.25 m. The principle of the model is the cell-by-cell mass balance calculated at each time step. The change in the water level in the cell in time is controlled by the surface water balance equation:

$$\frac{dh}{dt} = q_{in} + ep - (q_{in} + inf), \quad (1)$$

where h stands for surface water level [L], q_{in} and q_{out} for sheet overland inflow in and outflow from a given raster cell [L T^{-1}], *ep* for effective precipitation [L T^{-1}] and for *inf* for infiltration rate [L T^{-1}]. The kinematic wave approach is used in the calculation. The momentum is expressed by the power law:

$$q = ah^b, \quad (2)$$

where a and b are power-law parameters. Equation (2) can be expressed in the form of the Manning-Strickler formula

$$q = 1/ni^Y h^b, \quad (3)$$

where n and Y represent empirical parameters and i represent surface slope [−]. In this paper, we use Y and b to be equal to the Manning formula; $Y = 0.5$ and $b = 2/3$ (Manning, 1891).

The infiltration component of Equation (1) is calculated using Philip's infiltration equation (PHILIP, 1957).

$$inf = 1/2St^{-1/2}K_s, \quad (4)$$

where S stands for sorptivity [L $T^{1/2}$] and K_s for saturation hydraulic conductivity [L T^{-1}].

Table 2. Number of crop cover types of all artificial rainfall experiments.

Cultiv. bare soil	Corn	Green peas	Sorghum	Sunflower	Winter rape	Winter rye
40	18	2	17	4	3	1

The SMODERP2D model is subjected to uniform rainfall. Potential precipitation is reduced as a result of surface retention. Surface retention is a storage that must be filed before surface runoff may occur. The effective precipitation *ep* is defined as

$$\text{ep} = \begin{cases} 0 \; if \; ret \; \geq \sum_{i=t_0}^{t} p_i \\ p \; if \; ret \; \leq \sum_{i=t_0}^{t} p_i \end{cases}, \quad (5)$$

The flow routing of the surface runoff is based on the one direction flow algorithm D8 (O'Callaghan and Mark, 1984). The inflow to cell *i* is defined as a sum of sheet outflows from adjacent cells as

$$q_{in,i} = \sum_j^m q_{out,j}, \quad (6)$$

where j represents the index of adjacent upslope cells identified by the D8 flow algorithm.

The time derivative in Equation (1) is calculated using an explicit method. Therefore, the computation is sensitive to the time step size. The time step size is controlled with the Courant criterion, which needs to be kept below theoretical maximum value 1 or in practice even lower than 1 (Esteves et al., 2000; Zhang and Cundy, 1989).

The next time t + 1 step in Equation (1) with incorporating sum (6) is calculated for cell *i* as:

$$h_i^{t+1} = h_i^t + dt\left(\sum_j^m q_{out,j} + ep_i^t - q_{out,i}^t + inf_i^t\right). \quad (7)$$

The computational domain was based on the shape of the tiling flume of the rainfall simulator for all models. The plot area was discretized into 4 computational cells with equal area. The zero water level was set as an initial condition. No inflow was expected from the upper and end edges of the flume.

GLUE application

General likelihood uncertainty estimation (GLUE) was used to assess the uncertainty and sensitivity of models in the model ensemble. With this methodology, a model performance measure is used as a weight of model results and parameter sets which is then used to infer the uncertainty and sensitivity. The weighted model performance measure is normalized to express a likelihood of the given parameter set and model result. The common procedure consists of several steps that were principally followed in this paper (Beven and Binley, 1992). Usually, the Monte Carlo method is used to generate a set of model runs. Each model run is classified as behavioural and non- behavioural based on appropriate model performance measure and acceptance threshold of the performance measure. Only behavioural models are selected for further analysis.

Behavioural model generation

Surface roughness *n* (Eq. 3), surface retention, and Philips equation (Eq. 4) parameters were optimized for each measurement. The heuristic global optimization method differential evolution DE (Storn and Price, 1997) implemented in the Python Scipy package (Virtanen et al., 2020) was used to generate model instances. DE was used in hydrological modelling in the past (e.g., Turunen et al., 2020). The advantage of the DE over the usually used Monte Carlo method is that it can explore parameters at closer Pareto front optimum (Madsen, 2000) and therefore produce behavioural models more efficiently. However, this increases the risk of leaving out some of the behavioural models if not used with caution (Beven, 2012).

As with most optimization techniques, the range of parameters must be provided. Table 3 shows the uniform distribution of parameters. The Mannings roughness range was set high to encompass all possible values. The upper limit of K_s was set at 60 mm/h, which was the rain intensity during all experiments. Higher K_s cannot be identified by this procedure, as all water infiltrated for K_s > 60 mm/h. The lower limit of K_s is somewhat arbitrary. The 1 mm/h limit represents a situation when all water runs off. Regarding S, the range is set wide to ensure that the model cannot omit outliers. Additionally, when using differential evolution, the range effectively narrows as the algorithm approaches the more optimal parameter values. The limits of surface retention range from no retention (if zero) to 0.5 mm retention, a reasonable value considering the surface was flattened prior to each experiment.

Table 3. The parameter range used for the differential evolution.

Parameter	Min	Max	Units
n	0.004	1	–
K_s	2.78E–07	1.67E–05	m/s
S	1.00E–08	1.00E–02	m/sqrt(s)
surf. retention	–0.005	0	m

A combination of sum of squares (sum of squares of the difference between observed and modelled values) for the surface runoff and surface water level were combined as the objective function for DE:

$$SS = SS_h + w\,SS_q, \quad (8)$$

where *SS* stands for the total sum of squares, SS_h for the sum of squares calculated from the observed and modelled surface water level [m], and SS_q for the sum of squares calculated from the observed and modelled surface runoff [$m^3\ s^{-1}$]. The *w* stands for the weight factor that compensates for the different orders of magnitude between the SS_h and *SSq* and to prescribe some extra weight to the surface runoff which is of a more certain quality compared to the surface water level (calculated from the uncertain surface water flow velocity). *w* was set to 100 for all model runs.

During the DE calculation, all model runs with parameter sets were stored. In this paper, we used surface runoff and surface water level to optimize the models. Therefore, surface-runoff-based and water-level-based performance measures were calculated separately as well as its combination. The general formula of the model performance measure can be expressed as:

$$PM_x = (\sigma_{x,e}^2)^{-N}, \quad (9)$$

where PM is the model performance measure, σ_e^2 is a square of model residuals, and *N* is the parameter that sets the same value of the PM measure if set to 0 and assigns 1 to single best model if set to infinity. *N* was set at 0.1 in the presented study to produce reasonable wide 5 and 95% percentile of the likelihood measure (explained bellow) with respect to the measured data range. *x* could be *h* for the water-level-based model performance measure and *sr* for the surface-runoff-based model performance measure. In those cases, the square of residuals is calculated either from water level observed and modelled data or from surface runoff observed and modelled data.

For the combined model performance measure (PM), formula (9) has to be slightly altered:

$$PM_{all} = (\sum_{i=\{h,dis\}} \frac{w_i}{\sigma_{i,e}^2})^N. \quad (10)$$

Here W_i is the weight of observation i such that $\sum_{i=\{h,sr\}} W_i = 1$.

To choose the behavioural modes, a threshold has to be set above which the model is considered. As stated in (Beven and Binley, 2014), the threshold is a fuzzy number, since the transition between behavioural and non-behavioural models is continuous. In this study, we chose relaxed threshold to be equal to 25% percentile of the performance measure since DE is choosing models which tent to be closer to observations and to ensure that most of the measured data would fall within the uncertainty bonds (Freer and Beven, 2000).

Sensitivity analysis

A cumulative likelihood (normalized PM values) can illustrate the sensitivity of a single model to a specific parameter, as demonstrated, for example, in Freer and Beven (2000). This principle involves comparing the cumulative likelihood of the given parameter values with its prior distribution. If the cumulative likelihood closely resembles the prior distribution, the model exhibits low sensitivity to that parameter. Conversely, if the model's cumulative likelihood deviates significantly from the prior distribution, it indicates sensitivity to the parameters. Furthermore, the sharper the increase in cumulative likelihood, the higher the sensitivity of the model to the parameter.

The cumulative likelihood is obtained by normalizing and sorting PM obtained from Eq. (9) or (10). In this procedure, a curve resembling a statistical distribution is created showing the best performing parameter set with the highest likelihood. Using Eq. (9) in the analysis, a sensitivity of water level and surface runoff can be assessed separately. Using Eq. (10) overall sensitivity is assessed.

Uncertainty analysis

Similar to sensitivity analysis, a normalized sorted likelihood of the behavioural model is calculated for each realization of the model of each experiment for uncertainty analysis. The normalized likelihood median and the 5 and 95% percentile are calculated for each time step (each 60 seconds in the case of this study). The uncertainty is measured by the width of the 5 to 95% interval; the wider the range, the more uncertain the model results for that specific time step.

In addition, a median likelihood value of each parameter can be obtained. With this procedure an uncertainty of each parameter across the model ensemble can be assessed. It is worth noting that in the GLUE methodology, a unique set of parameters is always obtained. Therefore, the median value of one parameter does not have to be in the same parameter set with the median value of other parameters.

RESULTS AND DISCUSSION

Artificial rainfall simulations

Figure 2 shows the measured data used for the sensitivity and uncertainty analysis, demonstrating the range of the measured values to which the model realizations are compared. Generally speaking, the water level values (calculated based on the surface flow velocity) exhibited high variability, although within a smaller range for the wet soil water initial conditions experiments (Figure 2D). The surface runoff measurements always exhibited higher values for the bare soil cover experiments compared to the vegetated soil surface. However, the lag time of runoff onset was shorter regardless of the soil surface cover type.

Model sensitivity

Figure 3 illustrates dotty plots for each parameter, representing both water-level-based and surface-runoff -based performance measures (PM). The model yielded high PM values across a broad spectrum of parameter combinations. For surface roughness n, higher PM values were associated with lower n values, although this effect was less pronounced for surface-

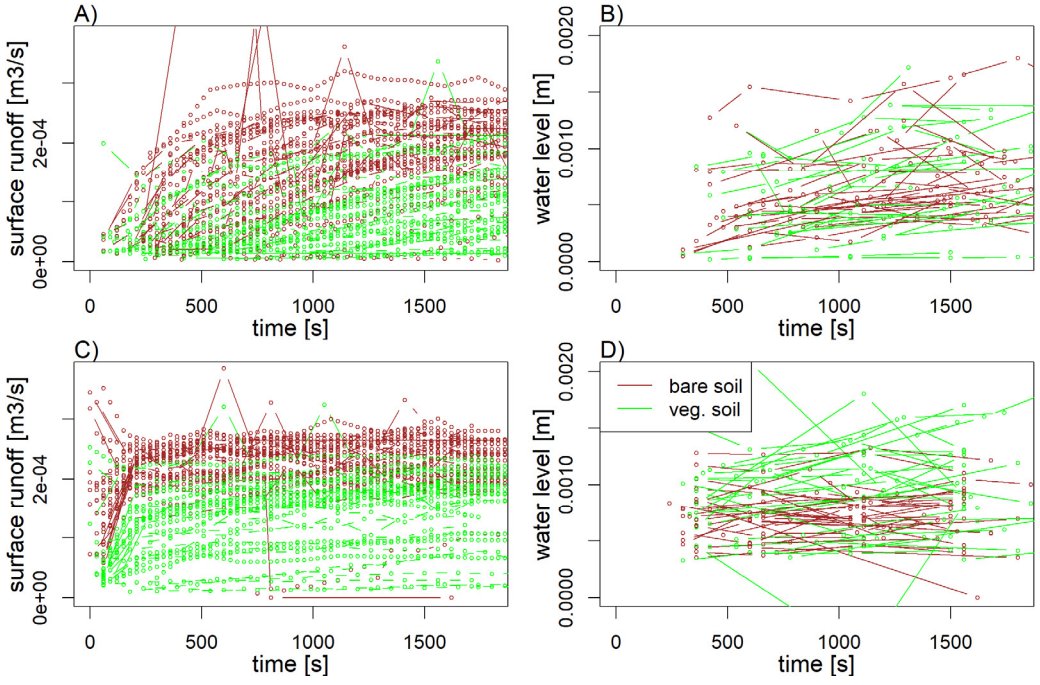

Fig. 2. Measured surface runoff (A, C) and surface water level (B, D) for dry initial soil water conditions (A, B) and we initial soil water conditions (C, D).

runoff-based PM, suggesting the sensitivity of the water level to surface roughness (Figure 3AE). On the contrary, K_s yielded higher PM values above 10^{-5} m/s for surface-runoff-based calculations, a trend that was less visible in water-level-based PM (Figure 3BF). K_s also showed an inverse pattern compared to n. Additionally, surface-runoff-based PM exhibited clearer peak than water-level-based PM for K_s suggesting less sensitivity in water level to K_s. Parameter S showed elevated PM values at 10^{-5} m/squared(s) for both PM variants (Figures 4CG). Surface retention displayed a wide range of values with consistently high PM, indicating that no specific values affected surface runoff or water level values; hence, low sensitivity of the

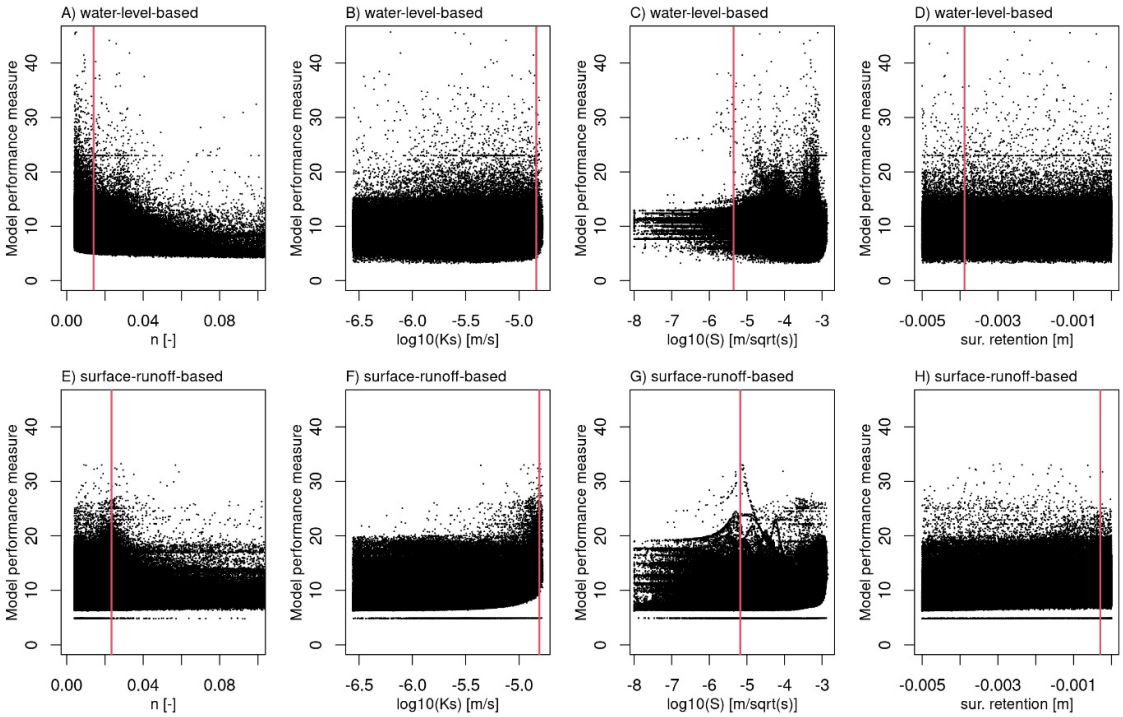

Fig. 3. Dotty plot of the performance measure for each model parameter. Plots A–D are inferred from the water-level-based performance measure. Plots E–H are inferred from the surface-runoff-based performance measure. The red line indicates the parameter value with the highest performance measure.

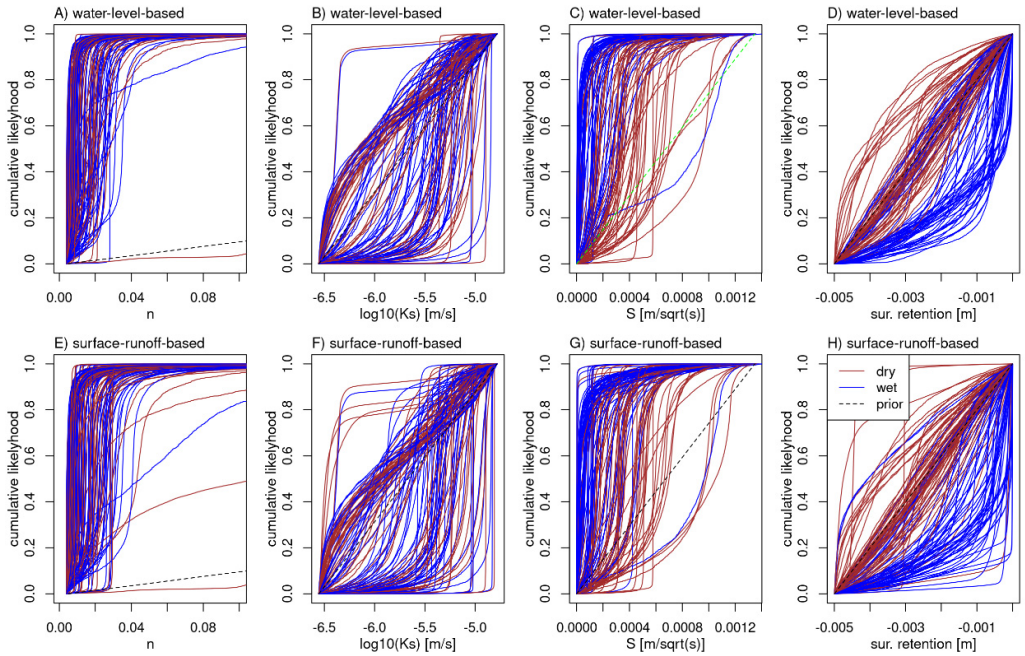

Fig. 4. Cumulative likelihood distribution for each model parameter for cumulative likelihood based on water level (top row) and cumulative likelihood based on surface runoff (bottom row). The colours indicate different initial soil water content, either wet (blue) or dry (red). The green dashed line indicates the cumulative likelihood of the uniform prior distribution (see Table 3).

model to surface retention. Overall, the absence of clear peaks in the dotty plots suggested a high degree of equifinality, similar to the water balance model in (Zhang et al., 2012).

The cumulative likelihoods based on water level and surface runoff did not show a clear difference, suggesting a similar sensitivity of the two variables to the model parameters (Figures 4 and 5). While individual models may demonstrate varying sensitivities across different modelled variables (Dohnal et al., 2012), this effect was observed only to a small extent in this study especially in dotty plot (Figure 3). Regarding individual parameters, the models showed sensitivity to surface roughness and sorptivity (Figures 4AE and 5AE), although this could be influenced by the wide range of the prior uniform distribution. The saturated hydraulic conductivity showed sensitivity in some models, as discussed below. The only parameter to which all models were least sensitive is the roughness of the surface (Figure 4DH and Figure 6DH).

The surface roughness sensitivity did not change when initial soil water content and soil cover were disturbed (Figure 4A and Figure 5E), highlighting the influence of the parameter to both the water level and the surface runoff calculations. Models were less sensitive to K_s for runs with bare soil surface conditions (Figure 4BF) due to high runoff with similar magnitude as the rainfall. Under such conditions, the surface runoff is controlled by rainfall rather than by K_s, causing low sensitivity of K_s. The initial soil water content did not affect the model's sensitivity to K_s (Figure 4BF). Model sensitivity to sorptivity did not show changes due to the initial water content or the type of soil cover, indicating its importance regardless of soil cover or soil water conditions (Figures 4CG and Figure 5CG). The insensitivity of the model to surface retention was the most pronounced under dry soil conditions (Figure 4DH). Under wet conditions, the soil surface is flattened by previous rainfall decreasing the water storage in surface depressions (Jeřábek et al., 2022); we remind that the wet initial soil water content experiments were performed after dry initial soil water conditions experiments. Therefore, surface retention is likely lower and the model is more sensitive to surface retention in wet initial soil water content models. Crop cover did not affect the model's sensitivity to surface retention (Figure 6DH).

Uncertainty analysis

For uncertainty analysis, we considered 25% of models with the lowest likelihood measure values as non-behavioural. The 25% cutoff value for behavioural models was calculated separately for each experiment. Since the likelihood based on surface runoff and water level does not show significant differences (Figures 4 and 5) the uncertainty analysis was evaluated using the combined likelihood PM_{all} (Eq. 9).

Uncertainty of model parameters

To further investigate parameter uncertainty, the median value of each parameter for each model can be determined from the cumulative likelihood curves. This median value can be considered as the optimal parameter value with the highest likelihood. Uncertainty of each parameter was assessed using the inter-quartile range (IQrR) and inter-quantile range (IQnR), which represents the parameter range between the 25th and 75th percentiles and 5th and 95th percentiles respectively.

Figures 6 and 7 depict the median values and uncertainty of the parameters in the model ensemble. Median surface roughness (n) values did not show a significant change in the initial soil water content (Figure 6A). However, noticeably higher median values of *n* were observed in model runs with cropped soil cover compared to bare soil model runs (Figure 7A). Furthermore, K_s values also showed significantly higher values under crop cover conditions (Figure 7B), while it showed insignificant differences for different initial soil water conditions.

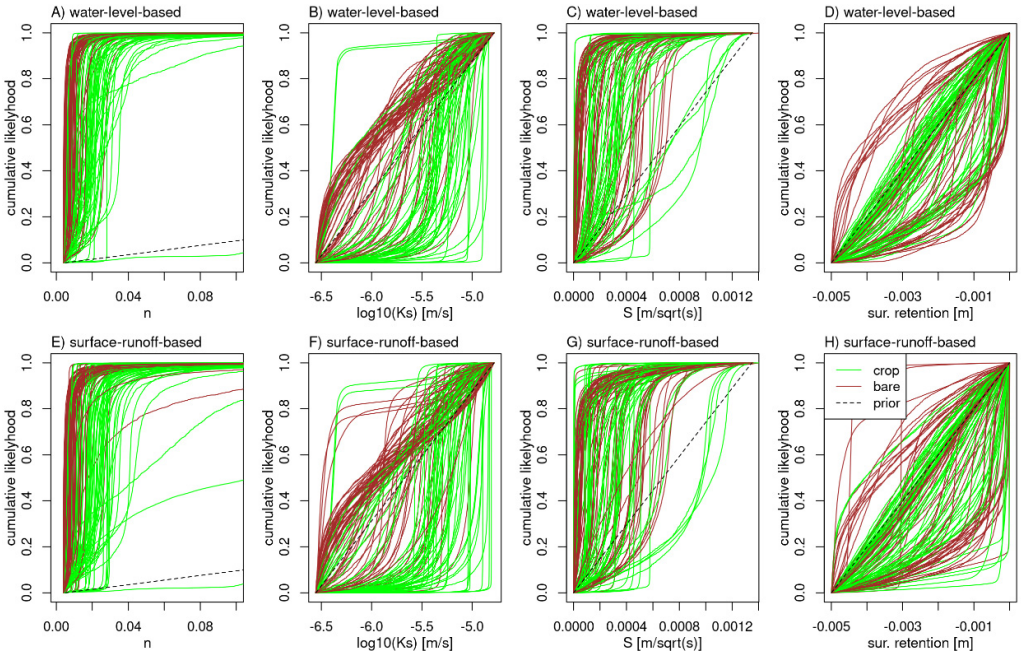

Fig. 5. Cumulative likelihood distribution for each model parameter for cumulative likelihood based on water level (top row) and for the surface-runoff-based cumulative likelihood based on surface runoff (bottom row). The colours indicate different soil cover, either bare (brown) or cropped (green). The green dashed line indicates the cumulative likelihood of the uniform prior distribution (see Table 3).

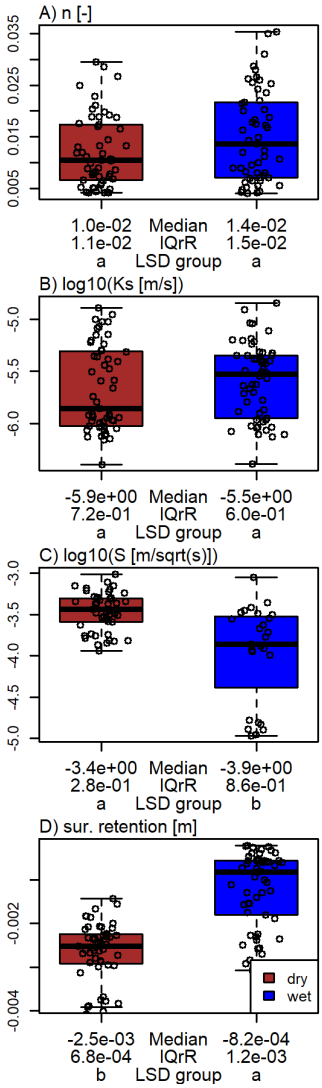

Fig. 6. Medial values for each parameter if the initial soil water content is distinguished. IQrRstands for inter quartile range. Brown boxplots depicts dry initial soil condition, while blue depicts wet initial soil water conditions.

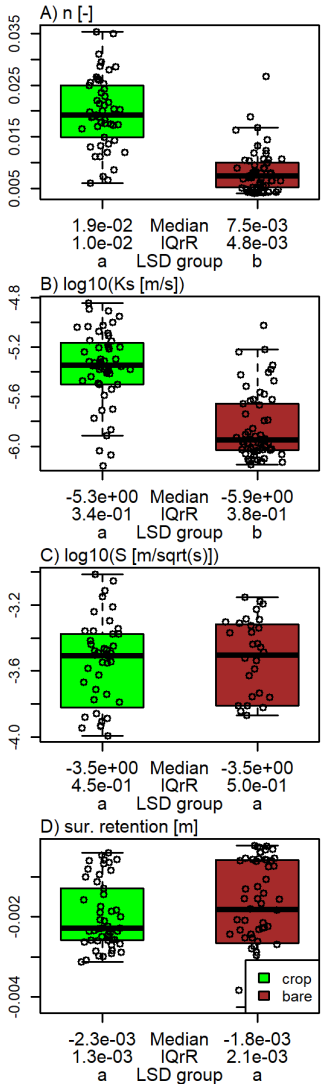

Fig. 7. Medial values for each parameter if the soil cover is distinguished. IQrR stands for inter quartile range. Green boxplots depict cropped soil surface, while brown depicts bare-soil soil-surface condition.

The uncertainty expressed as the interquantile range (IQrR) of parameter values did not show significant differences (Figures 6 and 7). IQrR was of the same order of magnitude for dry or wet conditions and for both bare soil and cropped model realizations. The only differences in the order of magnitude in IQrR were observed in surface retention for dry and wet initial soil content and for sorptivity under bare soil and cropped soil surface models. In contrast to (Schübl et al., 2023), weak correlation was observed between median and IQnR in most cases (Figure 8), with only a slight correlation found in surface roughness and sorptivity.

Surface roughness typically decreases with increasing rainfall, indicating a flatter surface under wet initial soil water conditions (Bauer et al., 2015). However, in this study, the surface roughness decreased due to the presence of crops (Figure 7A) rather than due to the flattening due to rainfall (Figure 6A). Additionally, the uncertainty in median roughness was higher in cropped soil surface models, possibly due to the effects of different stages of crop development or row width. However, the effect of flattening was compensated for in surface retention, where the models exhibited lower retention under initial wet soil water conditions (Figure 6D). This is probably due to the different scale the surface roughness and soil surface retention manifests. While, soil surface retention represents physical depressions in topography, roughness is property of surface regardless its curvature, which at studied scale did not change (Smith, 2014). Additionally, a more significant decrease in surface retention storage compared to the decrease in surface roughness was also observed in a study by (Jeřábek et al., 2022).

Crop cover may protect the soil surface from the impact that reduces the K_s (Haruna et al., 2018). Consequently, the effect of soil cover is more pronounced than that of the initial soil water content. Although the wet initial soil water content experiment followed the dry one, introducing soil surface sealing in the wet simulation. As demonstrated by Armenise et al. (2018), soil surface sealing can occur rapidly (in less than 14 minutes) in bare soil. This may result in the dry initial soil water content model runs to exhibit surface sealing for most of the experiments that causes K_s to be similar to the wet initial soil water content runs. Both soil surface roughness and saturated hydraulic conductivity

can decrease with increasing rainfall amount (Onstad et al., 1984), however after the 30 minutes of the dry initial soil water content experiments, we did not see a significant difference to wet initial soil water content experiments suggesting that the rainfall effect on reducing Ks and n occurred at the beginning of the dry initial soil water content experiments.

Neither the modelled sorptivity nor the surface retention median values showed variation due to different soil cover (Figure 7). For sorptivity, it was shown that the difference in pore size changes due to tillage (a seed ped preparation in the bare soil experiment) does not affect the sorptivity (Villarreal et al., 2017) which might be possibly the effect of the presented experiment. The median modelled sorptivity values exhibited lower values for the wet than for dry initial soil water condition experiments presumably because smaller pores were filled with water in the wet initial soil water content experiments, causing decreased sorptivity.

Furthermore, as shown in Figure 9, there is no correlation between any parameters. Unlike the parameter correlation observed in a single model, which shows redundancy in parameters, we demonstrate here that each parameter had its own role in the model across multiple models. This also indicates that the uncertainty of the parameters in the model set (the spread of the parameter median in each model) has a unique source.

Uncertainty in a single experiment

The GLUE methodology was applied to demonstrate the uncertainty in ensemble of surface runoff models. In the following section, the model uncertainty is depicted for each

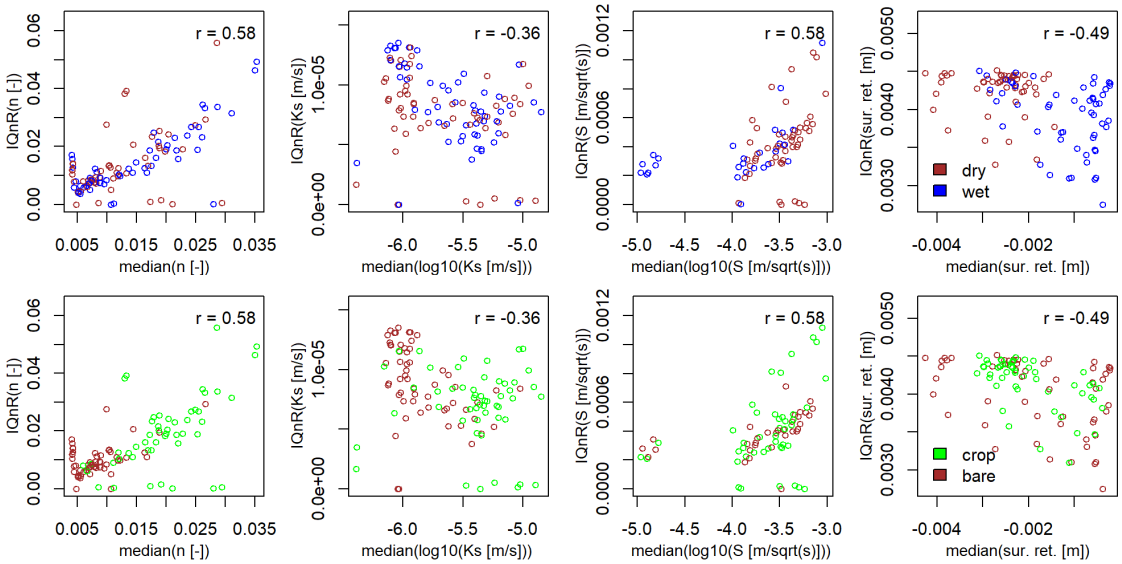

Fig. 8. Correlation between the median and IQnR (90% quantiles) of each parameter of each model. The upper and lower panels show identical data points with different colours to indicate the initial soil water conditions or the type of surface cover. r stands for the spearman correlation relationship.

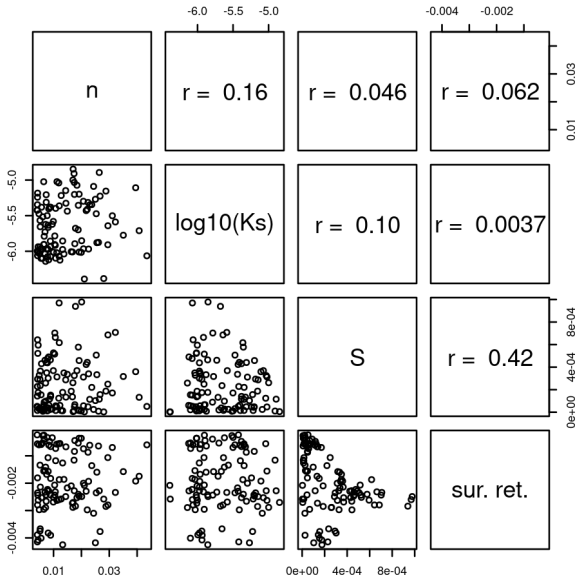

Fig. 9. Correlation between the median parameters of each model.

model separately, examining the most common modelling outcomes and their associated uncertainty. All graphs are presented in the supplementary data in Figures S1 to S8. Figures S1 to S4 illustrate model uncertainty in surface runoff, while Figures S5 to S8 depict uncertainty in surface water level.

The uncertainty was high in all experiments, as shown in Figure 10A for the surface runoff. While most median model values aligned well with observed surface runoff data, there were instances where the model entirely mismatched the observation, as illustrated in Figure 10B, or where the model overfitted the observations, resulting in very narrow uncertainty intervals (Figure 10C). These situations occurred randomly in simulations with dry initial soil conditions but were not observed in simulations with wet initial soil water content and were caused by initial parameter ques in the DE.

Overall, simulations with wet initial soil water conditions exhibited lower uncertainty in runoff lag time and better alignment with observed surface runoff values, as seen in Figures 10D and 10E due to shorter runoff lag time. However, experiments with wet soil initial conditions and cropped soil surfaces also showed decrease in uncertainty, despite some simulations showed a considerable lag time (Figure 10E). This led to counter intuitive suggestion, that vegetation cover decreased model uncertainty if compared to similar bare soil simulations.

Uncertainty in the model ensemble

To evaluate the uncertainty of the model ensemble for key hydrological variables, histograms were created for the surface runoff volume, runoff coefficient, maximum surface runoff, water level, and velocity in all behavioural models, as shown in Figure 11. We categorized the runs of the models by initial soil water content and soil cover.

The dry bare soil model runs exhibited the highest uncertainty (Figure 11), with the runoff volume and maximum surface runoff ranged within the whole physically possible range, as indicated by the runoff coefficient ranging between 0 and 0.8 (Figure 11). Interestingly, multiple modes were observed in the maximum surface runoff, indicating multiple models with similar maximum surface runoff. The maximum water level and the velocity of the water flow showed almost symmetric distributions. However, the potential critical velocity (which indicates the critical velocity for rill erosion occurrence (Kavka et al., 2022) was close to the modal velocity value. This uncertainty is particularly troubling, as rill erosion is one of the main causes of soil degradation, and the inability to model it with some degree of certainty is a major issue. The most probable causes of such high uncertainty in dry bare soil simulation were variability in soil surface morphology and initial soil water content, which may vary among dry experiments conducted in conditions affected by natural rainfall prior to the experiment.

Wet bare soil model runs showed narrower uncertainty with a tailing distribution toward lower values for water volume and maximum surface runoff. The soil was saturated and flattened by the precedent experiment, and almost 80% of the rainfall ran off. However, the maximum water level and, therefore, the maximum water flow velocity exhibited similar uncertainty in the wet and dry initial soil water conditions, indicating a preserved risk of initiating soil erosion. The difference in runoff

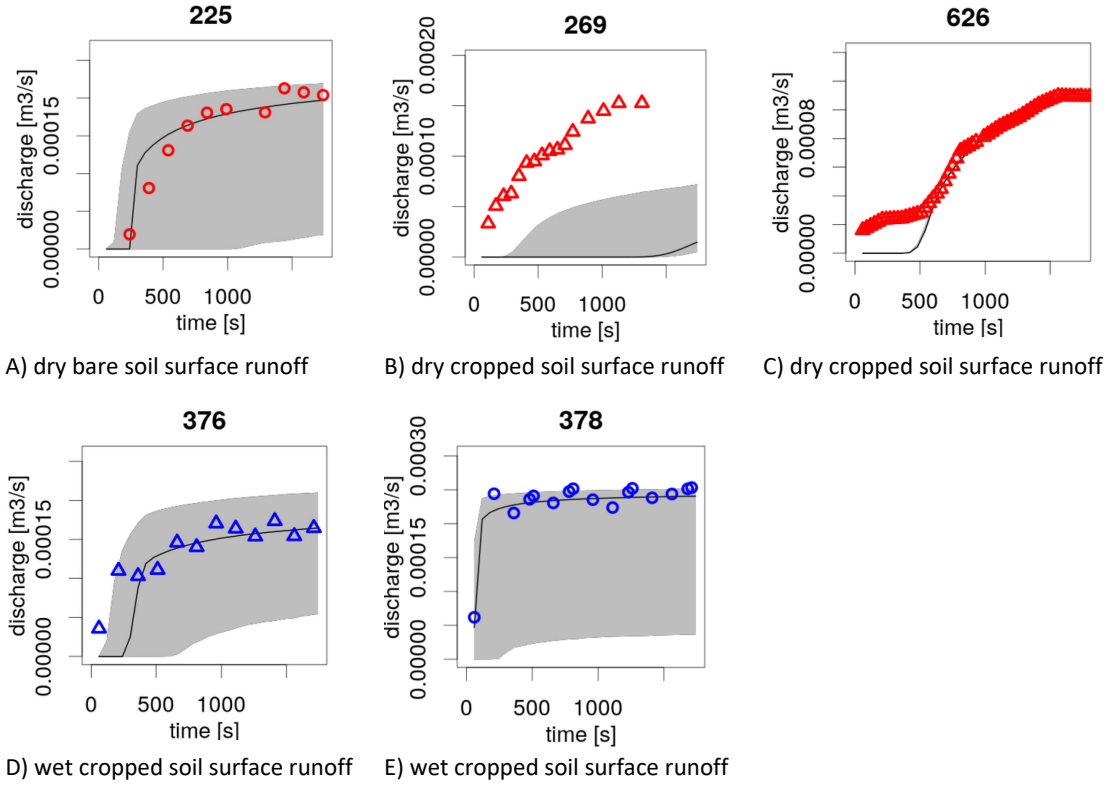

Fig. 10. Subset of experiments that represents a typical behaviour of the model ensemble. The full set of graphs is available in the supplementary materials (Figures S1–S8). The grey area represents the 90% uncertainty, black line the median model, the symbol shape represents the soil cover (circle for bare soil, triangle for cropped soil) and the symbol colour represents the initial soil water content (red for dry initial soil water content, blue for wet initial soil water content) of the measured data. Numbers above graphs indicate experiment ID in the from "An open rainfall-runoff measurement database" (Devátý et al., 2020).

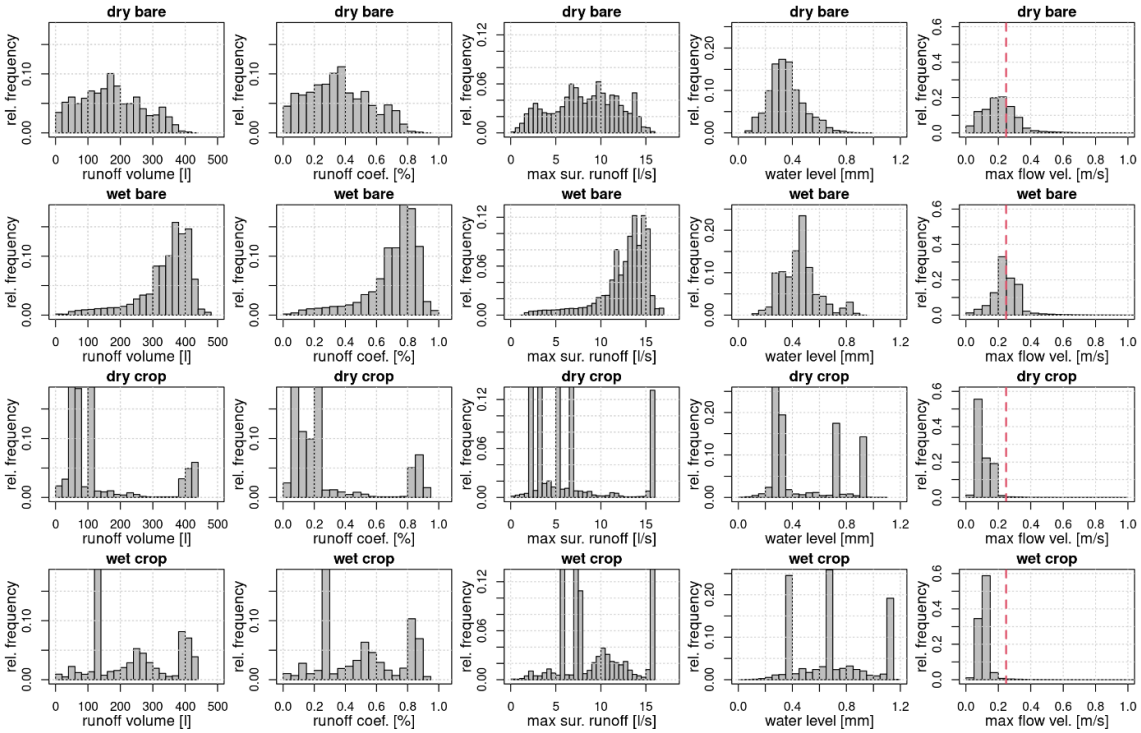

Fig. 11. Histogram of the median values of the model for cumulative surface runoff after [l] 30 minutes (fist column), runoff coefficient (second column), maximal surface runoff [l/s] after 30 minutes (third column), surface water level [m] (fourth columns) and maximal surface flow velocity [m/s] (fifth column). The dashed red line on the right panel represents the critical water flow velocity for sheet erosion for loam soil (v_{crit} = 2.480E–01 m/s, (Kavka et al*.,* 2024))

generation under different initial soil water content can be observed also in the catchment scale (Penna et al., 2011; Zumr et al., 2015). That can be explained with local and nonlocal runoff controls (Grayson et al., 1997). In the case of this study the nonlocal controls (vegetation, soil surface structure or infiltration properties; discussed below) were the potential cause of the higher uncertainty under dry initial soil water content conditions especially in bare soil models.

Model runs with a cropped surface exhibited high uncertainty. Multiple modes can be observed in both runs with dry and wet initial soil water content conditions. This is caused by a narrow uncertainty band, as shown in Figure 10C. It can be attributed to the DE, which in some cases was exploring parameters in a narrow range around initially good model performance. Also, each mode in histogram may attributed to different crop or crop stage. The only exception is the water flow velocity, which exhibited narrow. All behavioural model realizations fall below the critical water flow velocity, indicating a lowered erosion risk for cropped soil surface regardless of the specific crop type or stage of the crop's growth (Figure 11).

The high uncertainty in runoff volume and maximum runoff can be attributed to K_s, which is notoriously uncertain (e.g. (Baroni et al., 2010)). Under the dry initial soil water content condition, the sorptivity uncertainty had a stronger impact on the portion of the infiltrated water (Kubát et al., 2024) contributing to the overall water volume. A potentially large source of uncertainty in the runoff volume was surface retention that affected the runoff lag time. However, the model showed low sensitivity, and hence influence of surface retention to runoff volume uncertainty was debatable.

Uncertainty of the water flow velocity originated from routing of water on the soil surface, sometimes called surface connectivity. In reality, the water does not take the shortest downslope path, as is represented in the model (Jeřábek et al., 2022). Small irregularities on the surface of the soil expressed as surface roughness do not slow down water flow but rather prolong its path. As demonstrated in (Jeřábek et al., 2022) the water flow path of surface runoff can be 1.3 –1.7 times longer compared to the shortest slope wise path. This phenomenon, which is essentially caused by the organization of soil surface depressions, is usually omitted in hydrological models and brings a portion of the uncertainty. In the case of Figure 10 such uncertainty could be evaluated thanks to multiple repetition of similar experiment, where different pathways in measurements can be accounted for in the model ensemble since they occur in random manner.

CONCLUSIONS

Generalized Likelihood Uncertainty Estimation methodology was applied to study the sensitivity and uncertainty of the surface runoff model using an ensemble of artificial rainfall experiments. The ensemble consisted of experiments with similar setting allowing to study random effect such as: organization of soil surface, spatial heterogeneity of soil hydraulic properties or vegetation cover type and age on the model results and its uncertainty. The area of the experimental plot corresponds to the size of a single cell of the catchment scale model (~m^2) allowing to approximate the uncertainty in a single cell that would add up along the slope of the catchment scale model.

In particular, we showed that:

- Similar sensitivity of the modelled water level and surface runoff to all variables (with isolated exceptions). As a consequence, water level and surface runoff may be used interchangeably during e.g., optimization processes, allowing to choose easier to obtain variables.

- The model uncertainty is lower under wet initial soil water conditions. Conversely, our study showed that the dry initial soil water content uncertainty is particularly high especially with high lag time in the runoff onset models. This could produce uncertainty in the runoff coefficient in the range 0–0.8, emphasizing the importance of soil water content and its effect on runoff generation.

- Distinguishing vegetation stage and vegetation type in the model is necessary to decrease the uncertainty since water volume and runoff variables exhibited multiple modes that can be attributed to various crop and its age. However, the uncertainty under bare soil conditions was still higher for most variables.

- The setting of differential evolution (DE) algorithm is crucial. In some scenarios it may produce unrealistically narrow uncertainty bounds. Therefore, DE cannot be entirely automatic, and it always needs to be checked for various sets of parameter initial estimations. In contrast, this method can potentially reduce the amount of non-behavioural runs making the procedure more computationally efficient.

- We demonstrated high equifinality among the modelled experiments in the model ensemble.

This study further showed that any behavioural model of a small plot may or may not provide critical values of surface water flow that may indicate triggering of erosion. Therefore, if only a limited number of model runs are performed, the erosion risk situation may be overlooked. In such cases the situation must be assessed carefully since this uncertainty only increases for larger-scale models where the uncertainty shown in this study adds up along the water flow path.

The ensemble of artificial rainfall experiments showed high uncertainty in the surface runoff models caused by small-scale heterogeneity of soil properties, soil surface topography and vegetation variation. This uncertainty would remain hidden if only a single or even few experiments of rainfall-runoff episodes were used. The need of multiple repetitions of experiments or longer rainfall-runoff episodes is urgent. This is not always possible, especially in practice where scarce resources limit the possible date based for modelling. More research needs to be done to estimate how many experiments are necessary in order to stabilize the uncertainty bounds.

Acknowledgement. Presented work was done within project "LIVING LANDSCAPE" no. SFZP 085320/2022 funded by Norway Grants and provided by The State Environmental Fund of the Czech Republic. It was also supported by internal CTU student grant no. SGS23/155/OHK1/3T/11.

RERENCES

Armenise, E., Simmons, R.W., Ahn, S., Garbout, A., Doerr, S.H., Mooney, S.J., Sturrock, C.J., Ritz, K., 2018. Soil seal development under simulated rainfall: Structural, physical and hydrological dynamics. J. Hydrol., 556, 211–219. https://doi.org/10.1016/j.jhydrol.2017.10.073

Baroni, G., Facchi, A., Gandolfi, C., Ortuani, B., Horeschi, D., van Dam, J.C., 2010. Uncertainty in the determination of soil hydraulic parameters and its influence on the performance of two hydrological models of different complexity. Hydrol. Earth Syst. Sci., 14, 251–270. https://doi.org/10.5194/hess-14-251-2010

Bauer, T., Strauss, P., Grims, M., Kamptner, E., Mansberger, R., Spiegel, H., 2015. Long-term agricultural management effects on surface roughness and consolidation of soils. Soil Till. Res., 151, 28–38. https://doi.org/10.1016/j.still.2015.01.017

Benke, K.K., Lowell, K.E., Hamilton, A.J., 2008. Parameter uncertainty, sensitivity analysis and prediction error in a water-balance hydrological model. Math. Comput. Model., 47, 1134–1149. https://doi.org/10.1016/j.mcm.2007.05.017

Beven, K., 2012. Rainfall-Runoff Modelling. Wiley. https://doi.org/10.1002/9781119951001

Beven, K., Binley, A., 2014. GLUE: 20 years on. Hydrol. Process., 28, 5897–5918. https://doi.org/10.1002/hyp.10082

Beven, K., Binley, A., 1992. The future of distributed models: Model calibration and uncertainty prediction. Hydrol. Process., 6, 279–298. https://doi.org/10.1002/hyp.3360060305

Blasone, R.S., Vrugt, J.A., Madsen, H., Rosbjerg, D., Robinson, B.A., Zyvoloski, G.A., 2008. Generalized likelihood uncertainty estimation (GLUE) using adaptive Markov Chain Monte Carlo sampling. Adv. Water Resour., 31, 630–648. https://doi.org/10.1016/j.advwatres.2007.12.003

Boardman, J., Poesen, J., 2006. Soil Erosion in Europe. John Wiley & Sons, Ltd, Chichester, UK. https://doi.org/10.1002/0470859202

Brunetti, G., Šimůnek, J., Bogena, H., Baatz, R., Huisman, J.A., Dahlke, H., Vereecken, H., 2019. On the information content of cosmic-ray neutron data in the inverse estimation of soil hydraulic properties. Vadose Zone J., 18, 1–24. https://doi.org/10.2136/vzj2018.06.0123

Carpenter, S.R., Caraco, N.F., Correll, D.L., Howarth, R.W., Sharpley, A.N., Smith, V.H., 1998. Nonpoint pollution of surface waters with phosphorus and nitrogen. Ecol. Appl., 8, 559–568. https://doi.org/10.1890/1051-0761(1998)008[0559:NPOSWW]2.0.CO;2

Cho, S.J., Wilcock, P., Gran, K., 2022. Implementing landscape connectivity with topographic filtering model: A simulation of suspended sediment delivery in an agricultural watershed. Sci. Total Environ., 836, 155701. https://doi.org/10.1016/j.scitotenv.2022.155701

Cluckie, I.D., Xuan, Y., Wang, Y., 2006. Uncertainty analysis of hydrological ensemble forecasts in a distributed model utilising short-range rainfall prediction. Hydrol. Earth Syst. Sci. Discuss., 3, 3211–3237. https://doi.org/10.5194/hessd-3-3211-2006

Devátý, J., Beitlerová, H., Lenz, J., 2020. An open rainfall-runoff measurement database. EGU General Assembly 2020. Online. https://doi.org/10.5194/egusphere-egu2020-9148

Dohnal, M., Vogel, T., Šanda, M., Jelínková, V., 2012. Uncertainty analysis of a dual-continuum model used to simulate subsurface hillslope runoff involving oxygen-18 as natural tracer. J. Hydrol. Hydromech., 60, 194–205. https://doi.org/10.2478/v10098-012-0017-0

Dostál, T., Váška, J., Vrána, K., 2000. SMODERP — A simulation model of overland flow and erosion processes. Soil Eros., 135–161. https://doi.org/10.1007/978-3-662-04295-3_8

El Ghoul, I., Sellami, H., Khlifi, S., Vanclooster, M., 2023. Impact of land use land cover changes on flow uncertainty in Siliana watershed of northwestern Tunisia. Catena, 220, 106733. https://doi.org/10.1016/j.catena.2022.106733

Esteves, M., Faucher, X., Galle, S., Vauclin, M., 2000. Overland flow and infiltration modelling for small plots during unsteady rain: Numerical results versus observed values. J. Hydrol., 228, 265–282. https://doi.org/10.1016/S0022-1694(00)00155-4

Freer, J., Beven, K., 2000. Bayesian estimation of uncertainty in runoff prediction and the value of data: An application GLUE approach. Water Resour. Res., 32, 2161–2173.

Grayson, R.B., Western, A.W., Chiew, F.H.., 1997. Preferred states in spatial soil moisture patterns. Water Resour. Res., 33, 2897–2908.

Gupta, A., Govindaraju, R.S., 2023. Uncertainty quantification in watershed hydrology: Which method to use? J. Hydrol.,

616, 128749. https://doi.org/10.1016/j.jhydrol.2022.128749
Hantush, M.M., Kalin, L., 2005. Uncertainty and sensitivity analysis of runoff and sediment yield in a small agricultural watershed with KINEROS2. Hydrol. Sci. J., 50. https://doi.org/10.1623/hysj.2005.50.6.1151
Haruna, S.I., Anderson, S.H., Nkongolo, N. V., Zaibon, S., 2018. Soil hydraulic properties: influence of tillage and cover crops. Pedosphere, 28, 430–442. https://doi.org/10.1016/S1002-0160(17)60387-4
Holý, M., 1984. Vztahy mezi povrchovým odtokem a transportem živin v povodí vodárenských nádrží (dílčí zpráva výzkumného ústavu VI-4-15/01-03) Prague. (In Czech.)
Jeřábek, J., Zumr, D., Laburda, T., Krása, J., Dostál, T., 2022. Soil surface connectivity of tilled soil with wheel tracks and its development under simulated rainfall. J. Hydrol., 613, 128322. https://doi.org/10.1016/j.jhydrol.2022.128322
Kavka, P., Jeřábek, J., Landa, M., 2022. SMODERP2D – Sheet and rill runoff routine validation at three scale levels. Water (Switzerland), 14, 327. https://doi.org/10.3390/w14030327
Kavka, P., Jeřábek, J., Landa, M., Pesek, O., 2024. SMODERP2D - reference manual and user guide [WWW Document]. https://doi.org/https://github.com/storm-fsv-cvut/smoderp2d-manual
Kavka, P., Jeřábek, J., Landa, M., Pešek, O., 2023. SMODERP2D - Distributed event-based model for surface and subsurface runoff and erosion [WWW Document]. https://github.com/storm-fsv-cvut/smoderp2d. URL https://github.com/storm-fsv-cvut/smoderp2d
Kavka, P., Strouhal, L., Jáchymová, B., Krása, J., Báčová, M., Laburda, T., Dostál, T., Devátý, J., Bauer, M., 2018. Double size fulljet field rainfall simulator for complex interrill and rill erosion studies. Stavební obzor - Civ. Eng. J., 27, 183–194. https://doi.org/10.14311/cej.2018.02.0015
Kubát, J.-F., Strouhal, L., Kavka, P., 2024. Estimation of infiltration parameters: The role of pedotransfer functions and initial moisture conditions. J. Hydrol., 633, 130954. https://doi.org/10.1016/j.jhydrol.2024.130954
Li, T., Jerabek, J., Zumr, D., Noreika, N., Dostal, T., 2021. Assessing spatial soil moisture patterns at a small agricultural catchment. In: 2021 IEEE International Workshop on Metrology for Agriculture and Forestry (MetroAgriFor). IEEE, pp. 279–284. https://doi.org/10.1109/MetroAgriFor52389.2021.9628588
Loosvelt, L., Pauwels, V.R.N., Cornelis, W.M., De Lannoy, G.J.M., Verhoest, N.E.C., 2011. Impact of soil hydraulic parameter uncertainty on soil moisture modeling. Water Resour. Res., 47, 1–16. https://doi.org/10.1029/2010WR009204
Madsen, H., 2000. Automatic calibration of a conceptual rainfall-runoff model using multiple objectives. J. Hydrol., 235, 276–288. https://doi.org/10.1016/S0022-1694(00)00279-1
Manning, R., 1891. On the flow of water in open channels and pipes. Trans. Inst. Civ. Eng. Irel., 20, 161–207.
Moges, E., Demissie, Y., Larsen, L., Yassin, F., 2021. Review: Sources of hydrological model uncertainties and advances in their analysis. Water (Switzerland), 13, 1, 28. https://doi.org/10.3390/w13010028
Nanding, N., Rico-Ramirez, M.A., Han, D., Wu, H., Dai, Q., Zhang, J., 2021. Uncertainty assessment of radar-raingauge merged rainfall estimates in river discharge simulations. J. Hydrol., 603, 127093. https://doi.org/10.1016/j.jhydrol.2021.127093
O'Callaghan, J.F., Mark, D.M., 1984. The extraction of drainage networks from digital elevation data. Comput. Vision, Graph. Image Process., 28, 323–344. https://doi.org/10.1016/S0734-189X(84)80011-0
Onstad, C.A., Wolfe, M.L., Larson, C.L., Slack, D.C., 1984. Tilled soil subsidence during repeated wetting. Transactions of the ASAE, 27, 3, 0733-0736. https://doi.org/10.13031/2013.32862
Penna, D., Tromp-van Meerveld, H.J., Gobbi, A., Borga, M., Dalla Fontana, G., 2011. The influence of soil moisture on threshold runoff generation processes in an alpine headwater catchment. Hydrol. Earth Syst. Sci., 15, 689–702. https://doi.org/10.5194/hess-15-689-2011
PHILIP, J.R., 1957. The theory of infiltration. Soil Sci., 83, 345–358. https://doi.org/10.1097/00010694-195705000-00002
Schübl, M., Brunetti, G., Fuchs, G., Stumpp, C., 2023. Estimating vadose zone water fluxes from soil water monitoring data: a comprehensive field study in Austria. Hydrol. Earth Syst. Sci., 27, 1431–1455. https://doi.org/10.5194/hess-27-1431-2023
Schwen, A., Bodner, G., Loiskandl, W., 2011. Time-variable soil hydraulic properties in near-surface soil water simulations for different tillage methods. Agric. Water Manag., 99, 42–50. https://doi.org/10.1016/j.agwat.2011.07.020
Shen, Z.Y., Chen, L., Chen, T., 2012. Analysis of parameter uncertainty in hydrological and sediment modeling using GLUE method: A case study of SWAT model applied to Three Gorges Reservoir Region, China. Hydrol. Earth Syst. Sci., 16, 121–132. https://doi.org/10.5194/hess-16-121-2012
Šimůnek, J., Van Genuchten, M.T., 1996. Estimating unsaturated soil hydraulic properties from tension disc infiltrometer data by numerical inversion. Water Resour. Res., 32, 2683–2696. https://doi.org/10.1029/96WR01525
Smith, M.W., 2014. Roughness in the Earth sciences. Earth-Science Rev., 136, 202–225. https://doi.org/10.1016/j.earscirev.2014.05.016
Storn, R., Price, K., 1997. Differential evolution - A simple and efficient heuristic for global optimization over continuous spaces. J. Glob. Optim., 11, 341–359. https://doi.org/10.1023/A:1008202821328
Turunen, M., Gurarslan, G., Šimůnek, J., Koivusalo, H., 2020. What is the worth of drain discharge and surface runoff data in hydrological simulations? J. Hydrol., 587, 125030. https://doi.org/10.1016/j.jhydrol.2020.125030
Vigiak, O., Sterk, G., Romanowicz, R.J., Beven, K.J., 2006. A semi-empirical model to assess uncertainty of spatial patterns of erosion. Catena, 66, 198–210. https://doi.org/10.1016/j.catena.2006.01.004
Villarreal, R., Soracco, C.G., Lozano, L.A., Melani, E.M., Sarli, G.O., 2017. Temporal variation of soil sorptivity under conventional and no-till systems determined by a simple laboratory method. Soil Tillage Res., 168, 92–98. https://doi.org/10.1016/j.still.2016.12.013
Virtanen, P., Gommers, R., Oliphant, T.E., Haberland, M., Reddy, T., Cournapeau, D., Burovski, E., Peterson, P., Weckesser, W., Bright, J., van der Walt, S.J., Brett, M., Wilson, J., Millman, K.J., Mayorov, N., Nelson, A.R.J., Jones, E., Kern, R., Larson, E., Carey, C.J., Polat, İ., Feng, Y., Moore, E.W., VanderPlas, J., Laxalde, D., Perktold, J., Cimrman, R., Henriksen, I., Quintero, E.A., Harris, C.R., Archibald, A.M., Ribeiro, A.H., Pedregosa, F., van Mulbregt, P., Vijaykumar, A., Bardelli, A. Pietro, Rothberg, A., Hilboll, A., Kloeckner, A., Scopatz, A., Lee, A., Rokem, A., Woods, C.N., Fulton, C., Masson, C., Häggström, C., Fitzgerald, C., Nicholson, D.A., Hagen, D.R., Pasechnik, D. V., Olivetti, E., Martin, E., Wieser, E., Silva, F., Lenders, F., Wilhelm, F., Young, G., Price, G.A., Ingold, G.L., Allen, G.E., Lee, G.R., Audren, H., Probst, I., Dietrich, J.P., Silterra, J., Webber, J.T., Slavič, J., Nothman, J., Buchner, J., Kulick, J., Schönberger,

J.L., de Miranda Cardoso, J.V., Reimer, J., Harrington, J., Rodríguez, J.L.C., Nunez-Iglesias, J., Kuczynski, J., Tritz, K., Thoma, M., Newville, M., Kümmerer, M., Bolingbroke, M., Tartre, M., Pak, M., Smith, N.J., Nowaczyk, N., Shebanov, N., Pavlyk, O., Brodtkorb, P.A., Lee, P., McGibbon, R.T., Feldbauer, R., Lewis, S., Tygier, S., Sievert, S., Vigna, S., Peterson, S., More, S., Pudlik, T., Oshima, T., Pingel, T.J., Robitaille, T.P., Spura, T., Jones, T.R., Cera, T., Leslie, T., Zito, T., Krauss, T., Upadhyay, U., Halchenko, Y.O., Vázquez-Baeza, Y., 2020. SciPy 1.0: fundamental algorithms for scientific computing in Python. Nat. Methods 17, 261–272. https://doi.org/10.1038/s41592-019-0686-2

Vrána, K., Váška, J., Dostál, T., 1996. Smoderp - uživatelský manuál. (in Czech).

Vrugt, J.A., Bouten, W., 2002. Validity of first-order approximations to describe parameter uncertainty in soil hydrologic models. Soil Sci. Soc. Am. J., 66, 1740–1751. https://doi.org/10.2136/sssaj2002.1740

Vrugt, J.A., ter Braak, C.J.F., Diks, C.G.H., Robinson, B.A., Hyman, J.M., Higdon, D., 2009. Accelerating Markov Chain Monte Carlo simulation by differential evolution with self-adaptive randomized subspace sampling. Int. J. Nonlinear Sci. Numer. Simul., 10, 273–290. https://doi.org/10.1515/IJNSNS.2009.10.3.273

Wang, L., Zhang, Y., Jia, J., Zhen, Q., Zhang, X., 2021. Effect of vegetation on the flow pathways of steep hillslopes: Overland flow plot-scale experiments and their implications. Catena, 204, 105438. https://doi.org/10.1016/j.catena.2021.105438

Zhang, D., Zhang, L., Guan, Y., Chen, Xi, Chen, Xinfang, 2012. Sensitivity analysis of Xinanjiang rainfall-runoff model parameters: A case study in Lianghui, Zhejiang province, China. Hydrol. Res., 43, 123–134. https://doi.org/10.2166/nh.2011.131

Zhang, W., Cundy, T.W., 1989. Modeling of two-dimensional overland flow. Water Resour. Res., 25, 2019–2035.

Zhou, R., Li, Y., Lu, D., Liu, H., Zhou, H., 2016. An optimization based sampling approach for multiple metrics uncertainty analysis using generalized likelihood uncertainty estimation. J. Hydrol., 540, 274–286. https://doi.org/10.1016/j.jhydrol.2016.06.030

Zumr, D., Dostál, T., Devátý, J., 2015. Identification of prevailing storm runoff generation mechanisms in an intensively cultivated catchment. J. Hydrol. Hydromech., 63, 246–254. https://doi.org/10.1515/johh-2015-0022

Received 17 April 2024
Accepted 19 August 2024

SUPPLEMENTARY MATERIALS

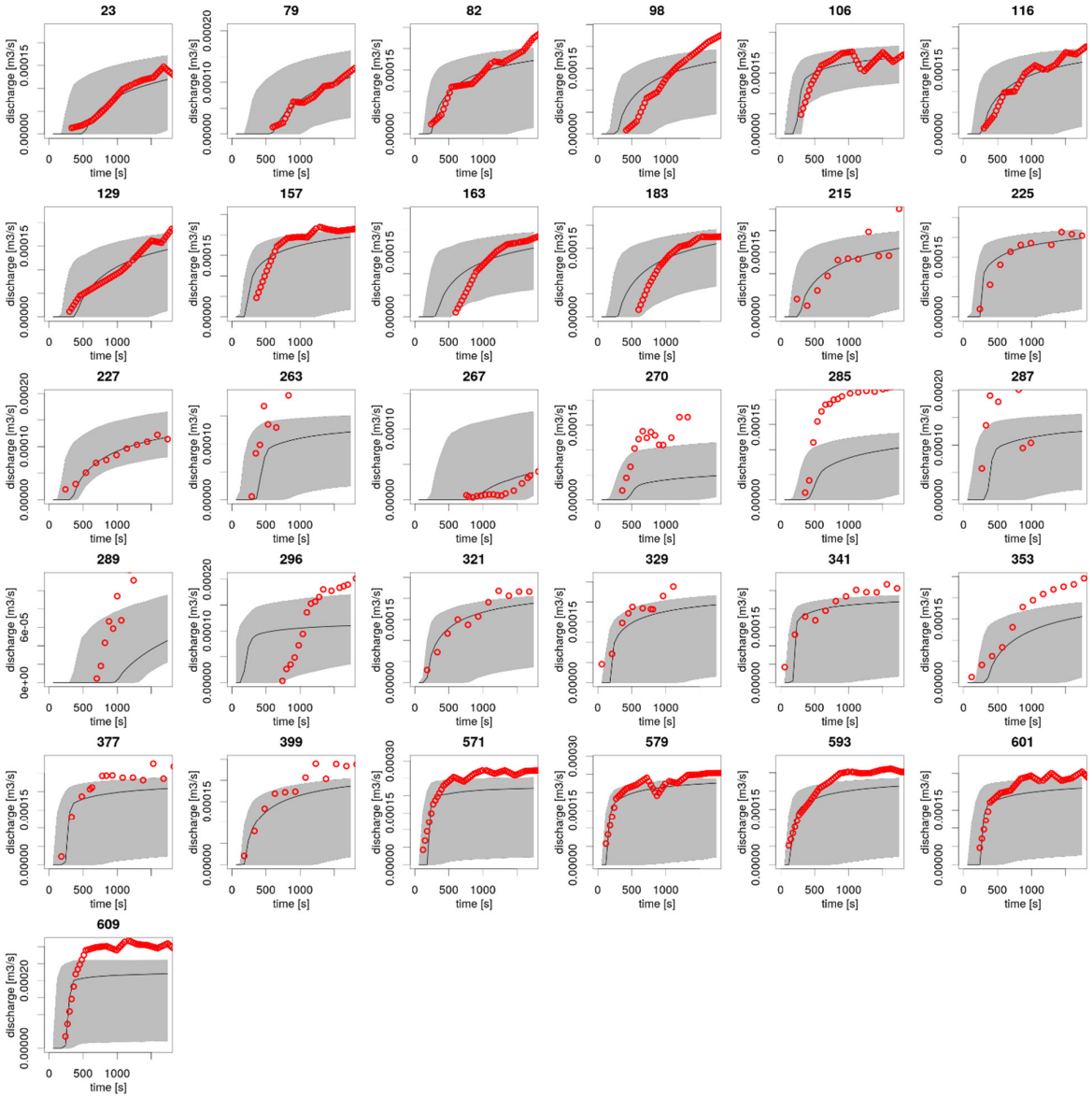

Fig. S1. The model median values (back line), uncertainty margins (grey area) and measured data (red circles) of discharge of models with dry initial soil conditions on bare soil. The grey area represents 90% margins.

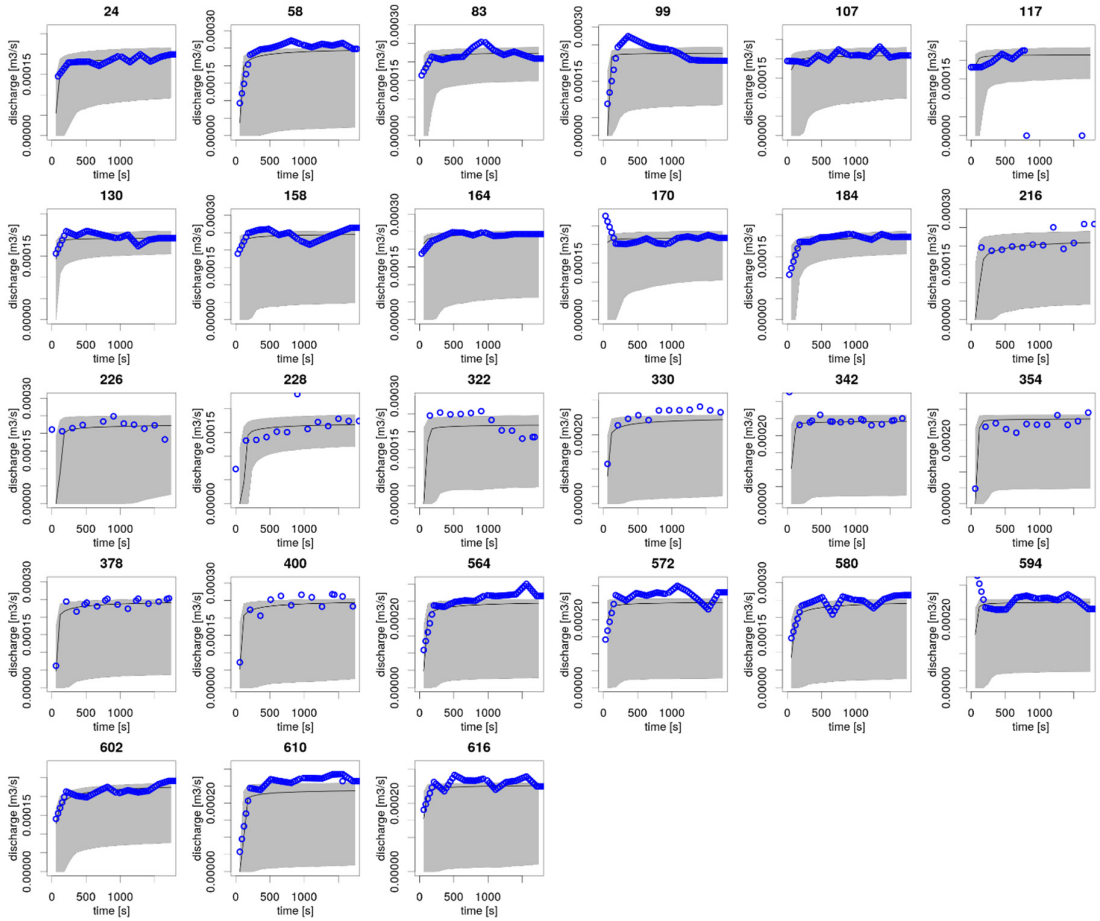

Fig. S2. The model median values (back line), uncertainty margins (grey area) and measured data (red circles) of discharge of models with wet initial soil conditions on bare soil. The grey area represents 90% margins.

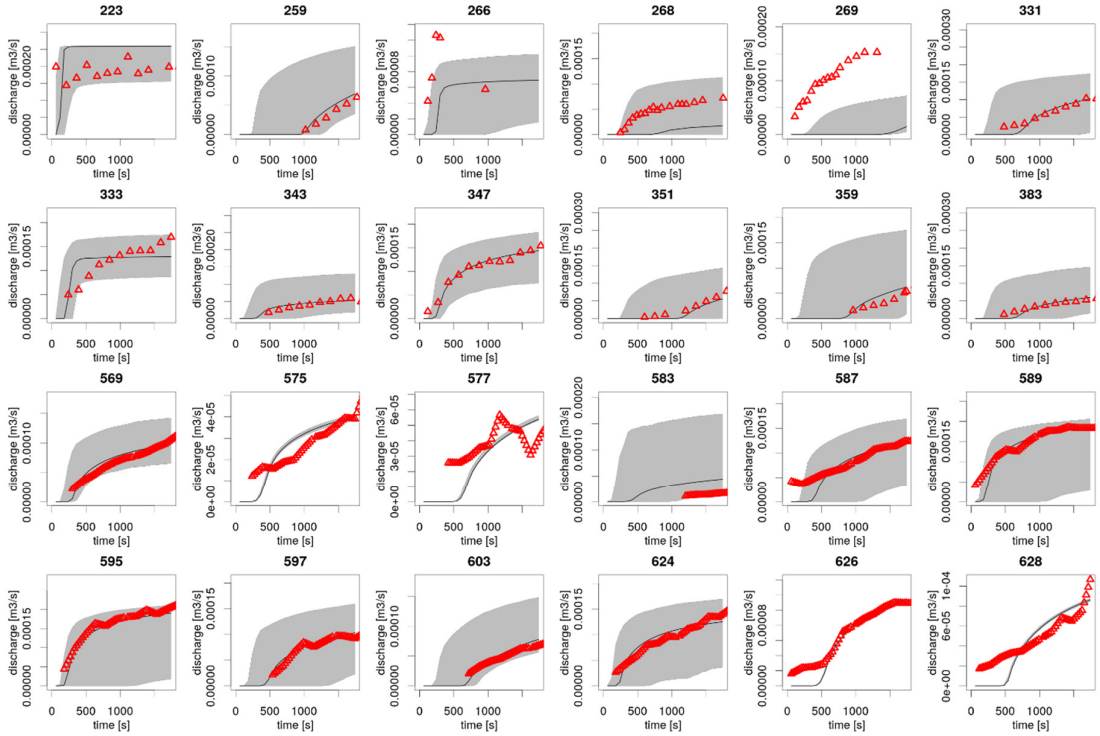

Fig. S3. The model median values (back line), uncertainty margins (grey area) and measured data (red triangles) of discharge of models with dry initial soil conditions on cropped soil. The grey area represents 90% margins.

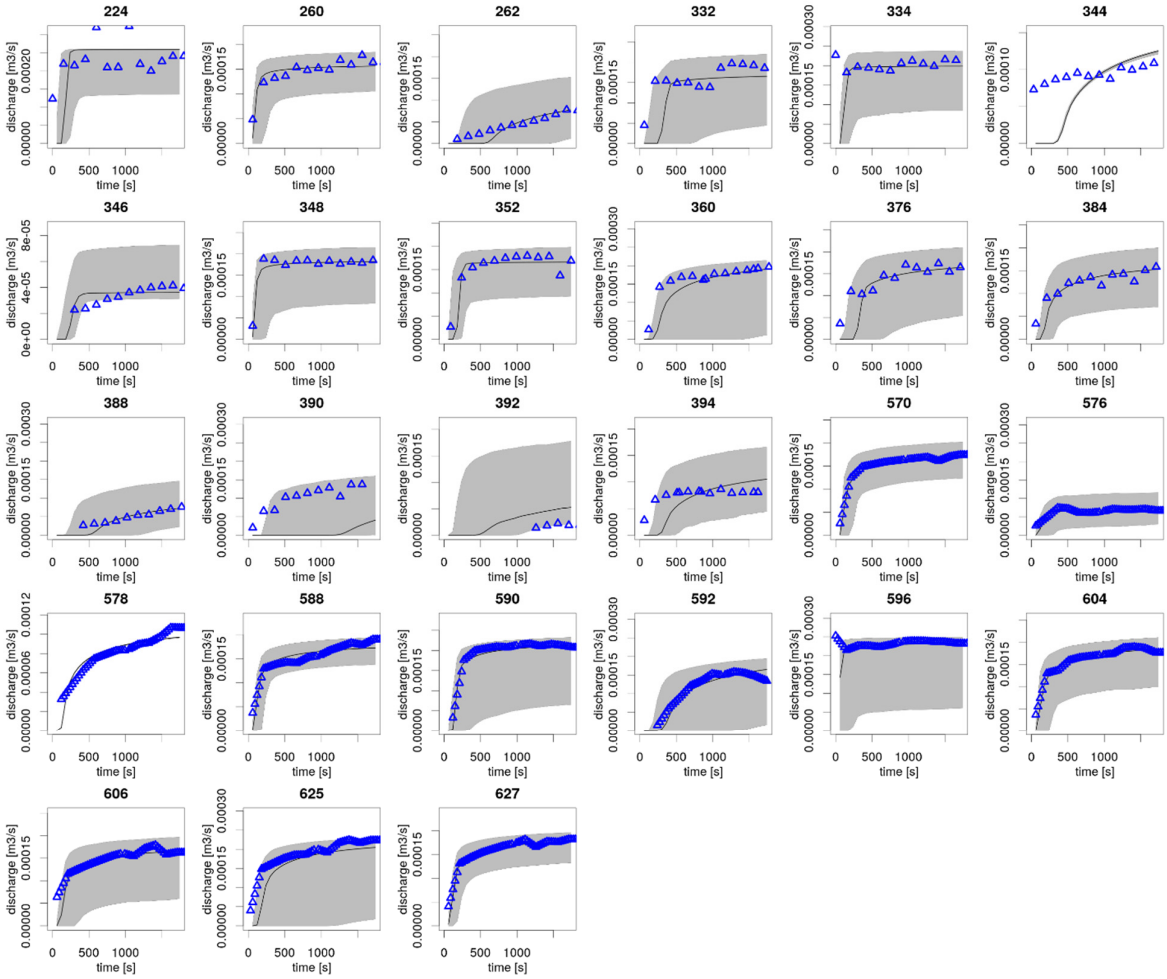

Fig. S4. The model median values (back line), uncertainty margins (grey area) and measured data (red triangles) of discharge of models with wet initial soil conditions on cropped soil. The grey area represents 90% margins.

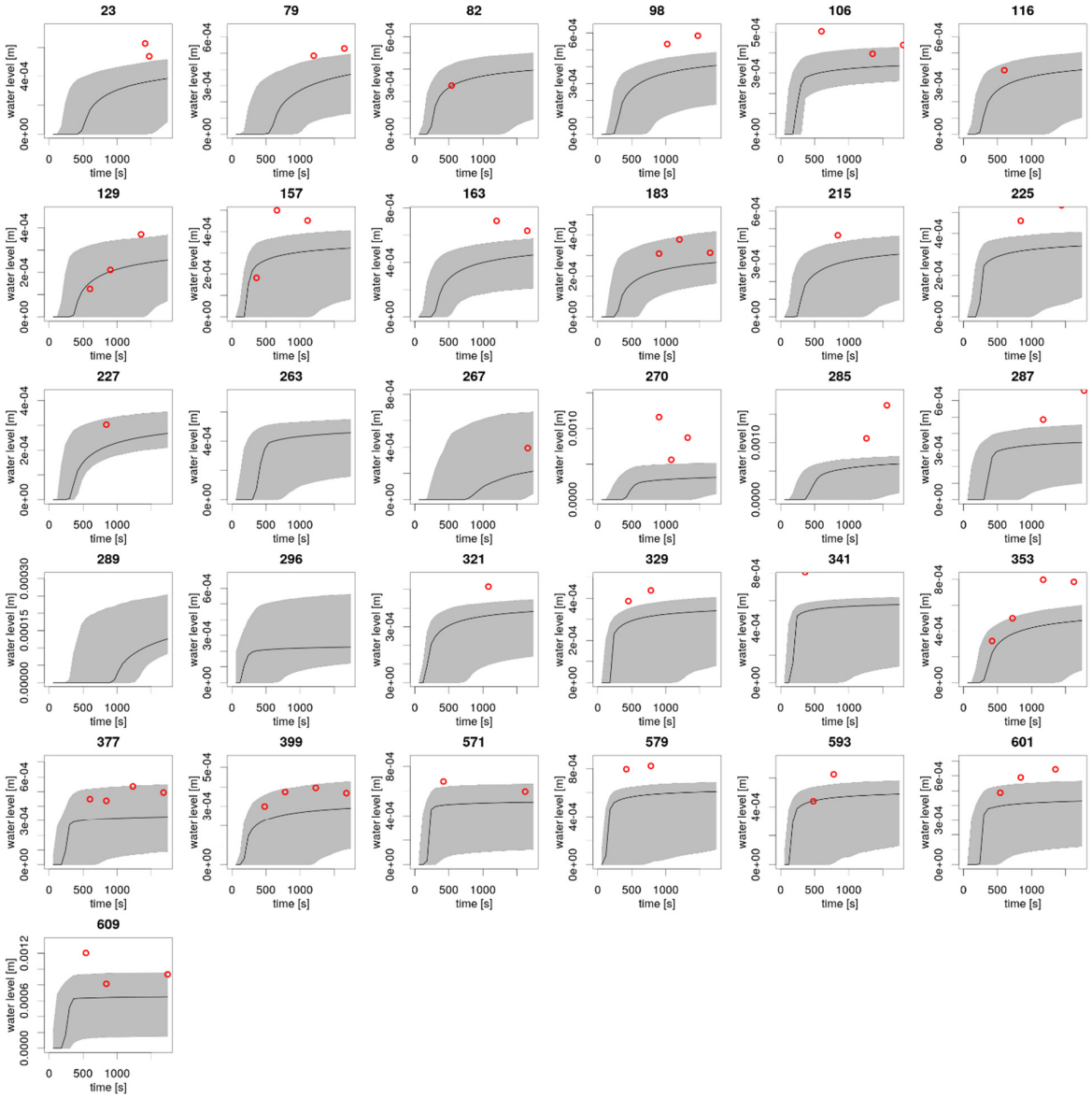

Fig. S5. The model median values (back line), uncertainty margins (grey area) and measured data (red circles) of water level of models with dry initial soil conditions on bare soil. The grey area represents 90% margins.

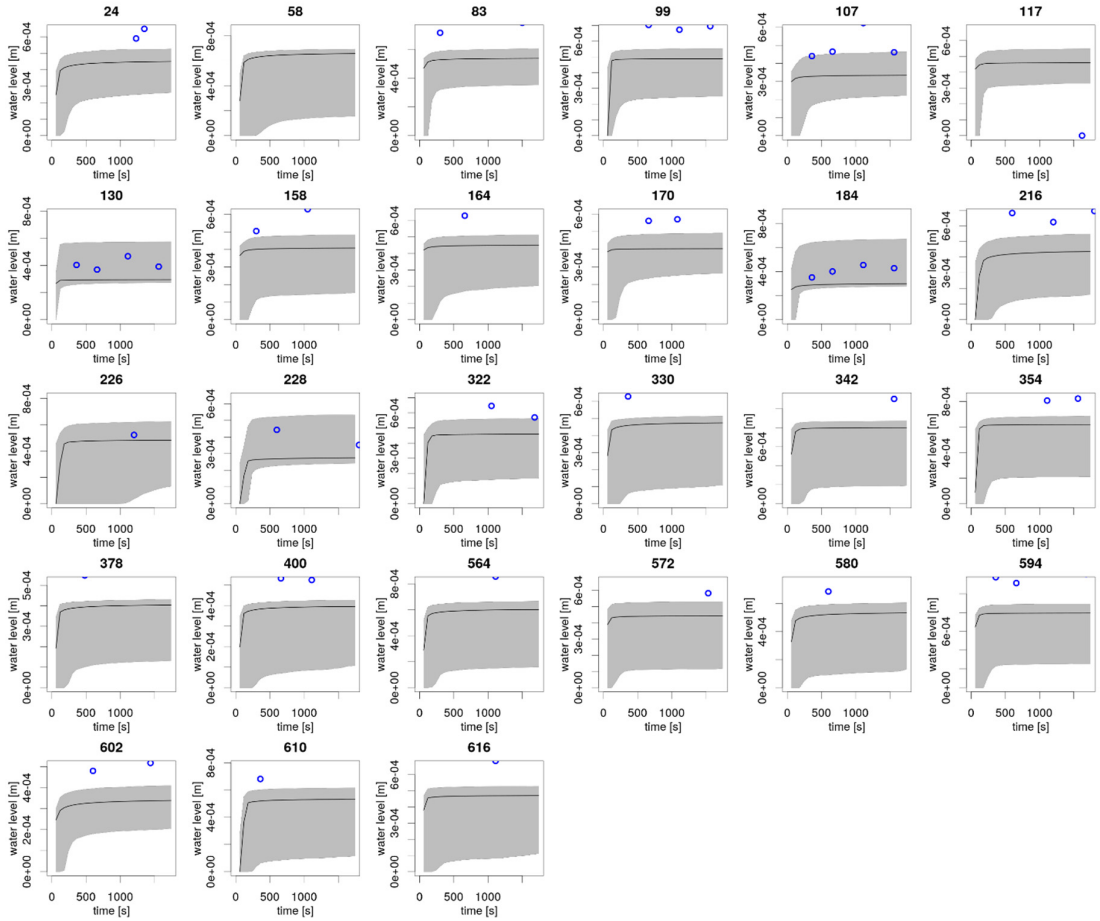

Fig. S6. The model median values (back line), uncertainty margins (grey area) and measured data (red circles) of water level of models with wet initial soil conditions on bare soil. The grey area represents 90% margins.

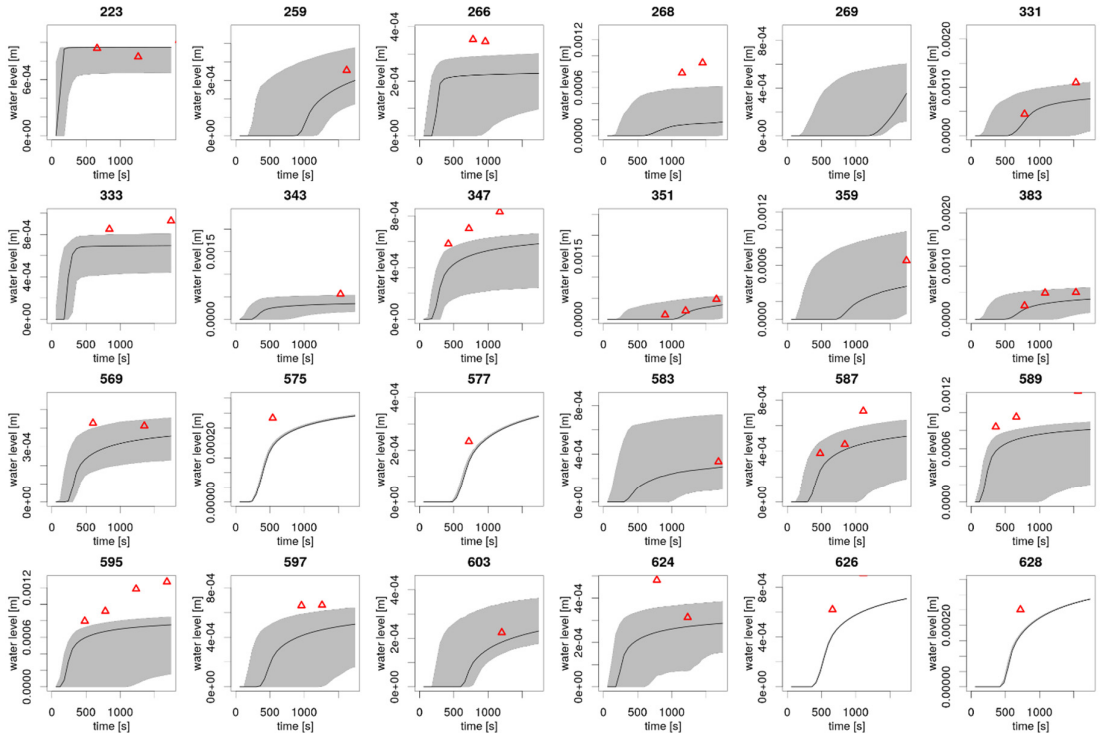

Fig. S7. The model median values (back line), uncertainty margins (grey area) and measured data (red triangles) of water level of models with dry initial soil conditions on cropped soil. The grey area represents 90% margins.

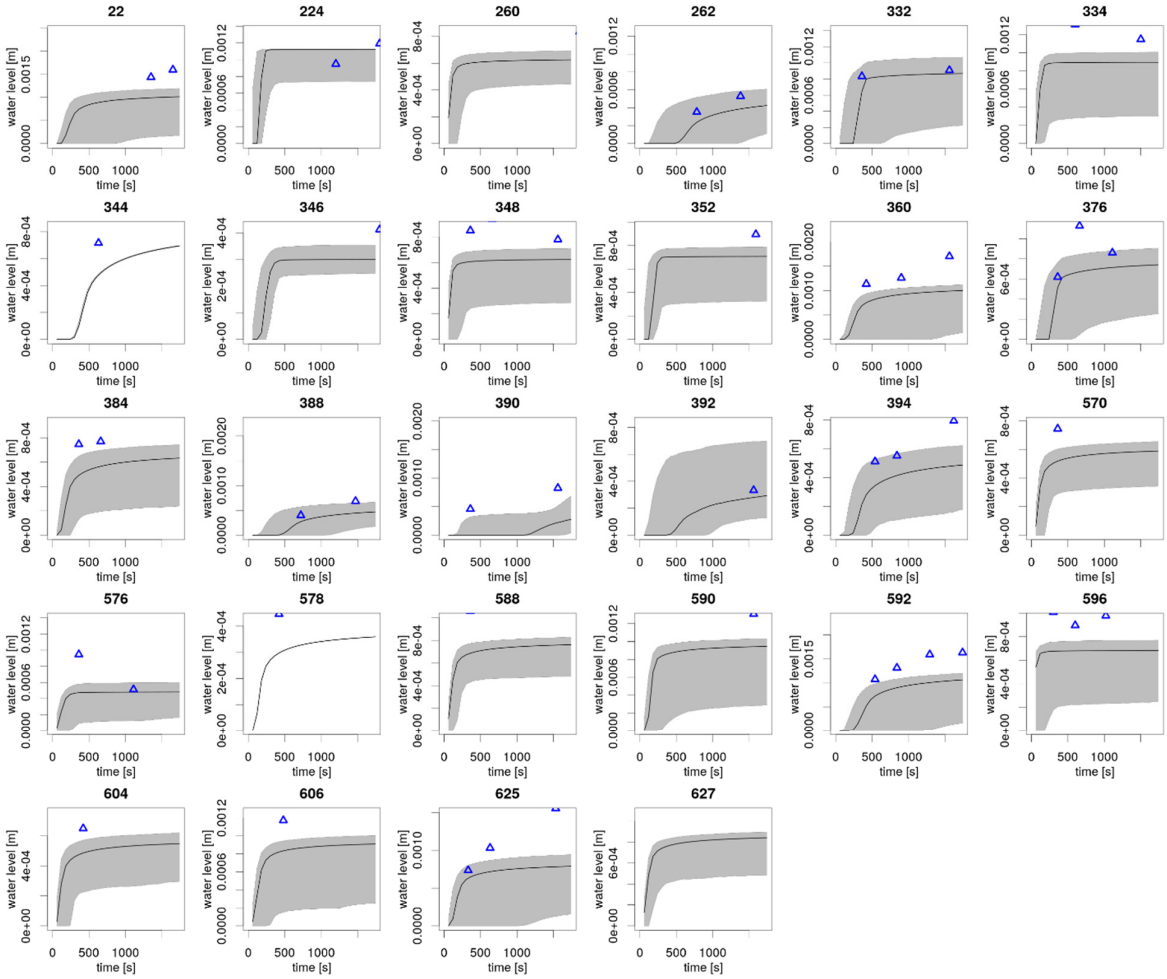

Fig. S8. The model median values (back line), uncertainty margins (grey area) and measured data (red triangles) of water level of models with wet initial soil conditions on cropped soil. The grey area represents 90% margins.